

Lidar wind speed measurements from a rotating spinner

Mikkelsen, Torben Krogh; Hansen, Kasper Hjorth; Angelou, Nikolas; Sjöholm, Mikael; Harris, Michael; Hadley, Paul; Scullion, Richard; Ellis, Gary; Vives, G.

Published in:
EWEC 2010 Proceedings online

Publication date:
2010

Document Version
Publisher's PDF, also known as Version of record

[Link back to DTU Orbit](#)

Citation (APA):
Mikkelsen, T., Hansen, K. H., Angelou, N., Sjöholm, M., Harris, M., Hadley, P., ... Vives, G. (2010). Lidar wind speed measurements from a rotating spinner. In EWEC 2010 Proceedings online European Wind Energy Association (EWEA).

DTU Library

Technical Information Center of Denmark

General rights

Copyright and moral rights for the publications made accessible in the public portal are retained by the authors and/or other copyright owners and it is a condition of accessing publications that users recognise and abide by the legal requirements associated with these rights.

- Users may download and print one copy of any publication from the public portal for the purpose of private study or research.
- You may not further distribute the material or use it for any profit-making activity or commercial gain
- You may freely distribute the URL identifying the publication in the public portal

If you believe that this document breaches copyright please contact us providing details, and we will remove access to the work immediately and investigate your claim.



LIDAR WIND SPEED MEASUREMENTS FROM A ROTATING SPINNER

T. Mikkelsen, K. Hansen, N. Angelou, M. Sjöholm
Risø DTU, Roskilde, Denmark
tomi@risoe.dtu.dk

M. Harris, P. Hadley, R. Scullion, G. Ellis, G. Vives
Natural Power, Malvern, UK
michaelh@naturalpower.com

Abstract:

We report our latest results from an experimental development in which a fast data acquisition continuous wave (cw) wind lidar (ZephIR) has been installed and operated in the rotating spinner of a large 80 m Ø, 59 m hub height wind turbine (Vestas NM80) located at Tjæreborg Enge in western Denmark. To the best of our knowledge we have achieved a "World first" successful operation of a forward-looking wind lidar integrated in the spinner of an operating wind turbine. This new measurement concept allows for an unimpeded view of the approaching wind field, which we have interrogated using several different wind scan patterns. Information on wind speed, shear and direction has been extracted and compared to the output from an adjacent met mast.

Keywords: Wind lidar, wind turbine integration, yaw and pitch steering and control, power curve.

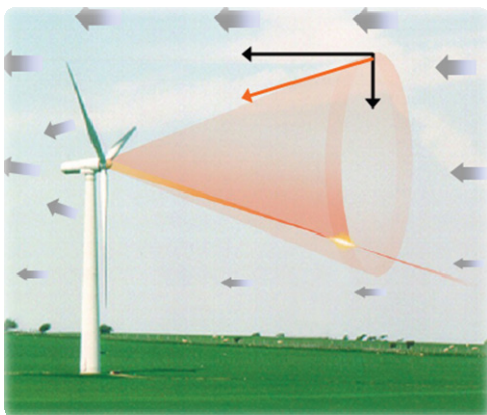


Figure 1: Concept of measuring the upwind inflow conditions from a lidar integrated in the tip of a rotating spinner.

1 Introduction

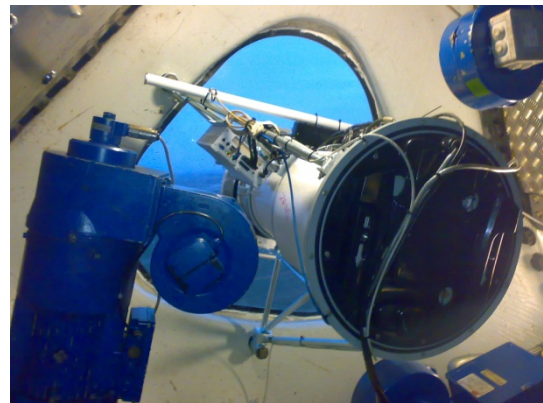


Figure 2: The cw lidar installed on the turbine axis in the tip of the NM80 spinner. The lidar measures the approaching wind conditions by conical scanning with the laser beam through the window. Also seen are the three pitch control motors (blue).

Laser anemometry (lidar) is capable of making detailed measurements of the wind field approaching the blades of operational wind turbines. Incorporation of advance wind data into the turbine control system offers the possibility of improved energy yield and load reduction [1]. A turbine-mounted lidar capability was first achieved in a proof-of-principle experiment in 2003, in which a prototype ZephIR lidar was placed on the nacelle of a Nordex N90 turbine [2].

The lidar stared through the blades of the turbine and demonstrated the feasibility of accurate wind speed measurements at ranges up to 200 m in front of the turbine blades. Since then a number of different lidar devices have become available for use in the wind industry, all based on optical fibre and other components developed originally for the telecommunications industry. This approach has

radically improved the cost, reliability and overall utility of lidar systems [3], and the technique now provides a genuine prospect for improvement of future turbine performance.

2 Lidar integration in spinner

2.1 Experimental setup

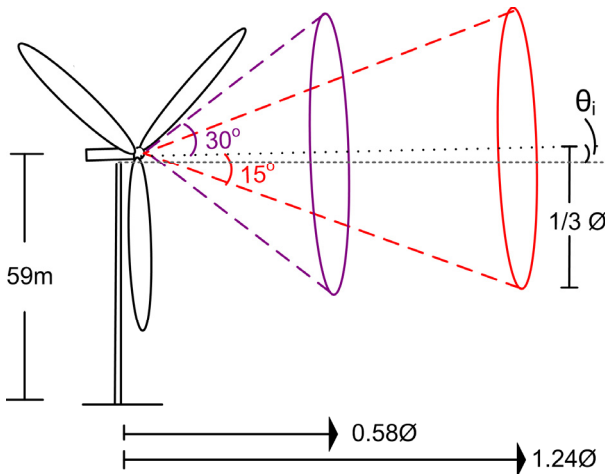


Figure 3: Representation of the geometry of the measurements, θ_i is the tilt angle of the turbine rotation axis.

The lidar was mounted in the tip of the rotating spinner and aligned with the turbine shaft axis (cf. Fig. 1 and 2). On-line real-time data access and lidar control was enabled via wireless telecommunication, cf. the white antenna in Fig.2.

Placing the lidar in the centre of a turbine proved difficult, because of the changing gravitation direction and centrifugal force generated by the turbine's rotation. Another problem that was overcome related to the electrical interference from the generator. The detector in the lidar is extremely sensitive and is easily upset by spurious currents. The detector and the most sensitive electronics were therefore wrapped with shielding material that conducts surplus electricity to earth.

While the turbine was operating, the lidar's built-in wedge scanned the incoming wind field in different circular scan patterns in the rotor plane, either 46 m or 100 m in front of the turbine, corresponding to 0.58 and 1.24 δ rotor diameters upwind along the turbine shaft axis.

The experimental setup was designed with scan cone half-angles of 15 degrees and 30 degrees in order to point and focus the lidar at the maximum lift $2/3$ blade cord radius, corresponding to a distance along the laser beam to the focus point of

53m with the 30 degree scanning angle cone and with 103 m distance to the focus point with the 15 degree cone, respectively, cf. Fig. 3.

2.2 Data streaming and processing

The scan azimuth angle with respect to a fixed coordinate system is calculated from recorded information from the lidar's rotating wedge scanner and from measurements of the wind turbine's rotor position. With co-rotating wedge and rotor, a full 360-degree cone scan was performed in about 0.8 s while wind speed Doppler spectra were streamed at a rate of 50 Hz to a PC adjacent to the lidar. We estimate the cw lidar's radial measurement resolution to be about 20 m (full width half-maximum) at the 103 meter range and about 5 m at the 53 m range [4]. The data have been post-processed to provide axial wind speed versus azimuth (scan) angle in non-rotating, fixed frames of reference.

3 Wind measurements

3.1 Upstream wind scanning

Figure 4 shows four examples of upwind inflow obtained from the wind lidar's azimuth scanning about the turbine axis. Data have been obtained in the rotor plane at the two investigated upwind distances located at approximately $2/3$ and at $4/3$ rotor diameter distances upwind respectively.

Wind speeds are presented in polar plots and the lidar-measured radial wind speeds have been projected along the turbine axis under the assumption that the wind fluctuations are small compared to the mean wind speed. The projection of the measured line-of-sight lidar data onto a coordinate system aligned with the pointing direction of the turbine is presented in Appendix A.

The polar plots below show wind speeds obtained with the 15-degree wedge during the night of April 30, 2009. The boundary layer was strongly stratified and the turbulence was accordingly representative for stable atmospheric conditions with sporadic outbursts of intermittent turbulence.

The processed data in Fig. 4 show a high degree of variability in the approaching wind field encountered here during intermittent and stable stratified atmospheric conditions. The plots show lidar-measured radial wind speeds. Each of the four plots show data from ten full 360-degree azimuth scans sampled during consecutive 8 s periods.

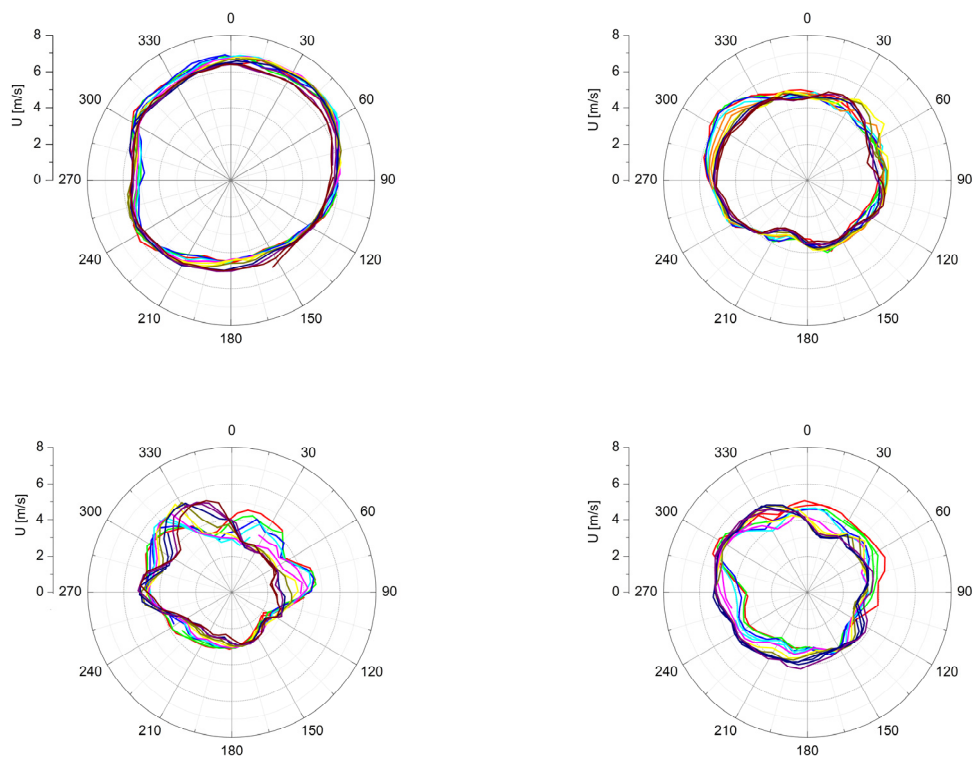


Figure 4: Four examples of spinner-lidar measured upstream wind speeds during the early morning on April 30, 2009. Each of the four plots contains ten consecutive 360-degree scans of the wind speed measured remotely 100 meters in front of the operating turbine. The zero scan angle is defined to be at the uppermost point of the conical scan pattern.

These, to our knowledge “World first” new data show, not surprisingly, that the approaching wind field contains turbulent coherent structures, many of which have dimensions comparable to the rotor plane, and which can prevail in time over several seconds. Assuming that the standard “Taylor’s frozen turbulence” hypothesis applies, this indicates that coherent structures in the turbulence will remain and impinge upon the rotating turbine blades a few seconds after they are detected.

The mean wind speed during the April 30th experiment ranged between 5 and 8 m/s meaning that the measured turbulent structures should reach the turbine within a time span of 12 – 20 seconds later. Such lead times provide ample possibility for pitch control of the blades to mitigate fatigue effects from strong wind shear and yaw errors and for optimising the power production via individual adjustments of pitch angles.

Fig. 5 shows spinner-measured axial projected wind speeds measured in the rotor plane similar to the data in Fig. 4 from the night time experiment April

30, 2009. Here, however, we present all the wind speeds sampled at 50Hz over a full 10-min period.

The measurements show that a strong vertical shear is present in the rotor plane, both with respect to direction and magnitude. In addition, the mean wind is not symmetrical in this case with respect to the turbine’s vertical axis. It is furthermore evident that there is more turbulence near the ground in this night-time stable stratified flow experiment.

In Fig. 6 an inter-comparison between the vertical wind profiles measured by the spinner-mounted lidar and a co-located met-mast is shown. It is noticed that the wind profiles are approximately linear with height, which is indicative of a strong stable stratified mean wind flow. The met mast was located approximately 300 meters downstream of the NM80 turbine during the night time data collection period of April 30. Therefore, wake effects in combination with a low boundary layer mixing height could sometimes be observed in the vertical profiles.

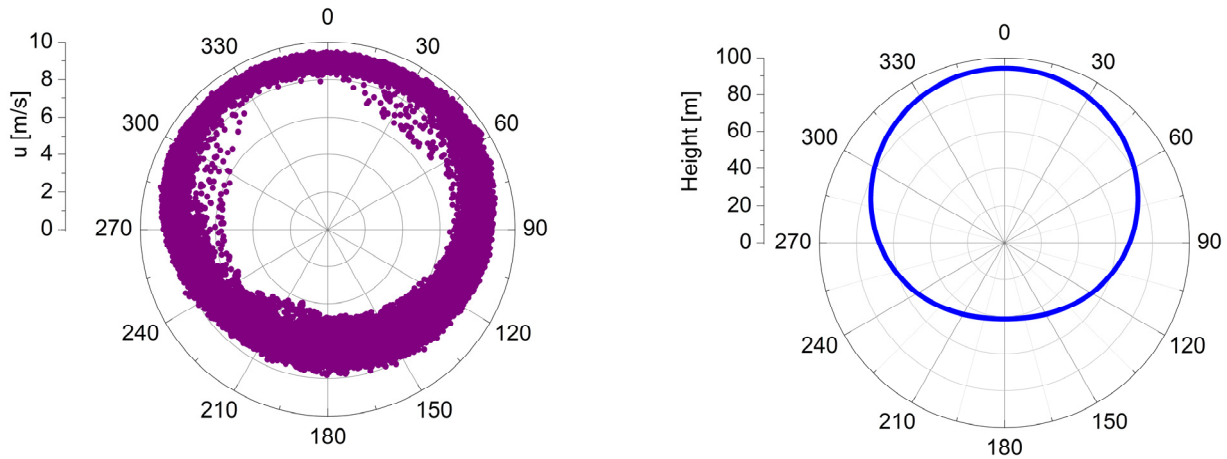


Figure 5: Left) Spinner-lidar measured upwind wind speed sampled during a 10-min period. Right) The lidar's measurement heights above ground level as a function of scan angle.

Nevertheless, as seen in Figure 6, good agreements could most of the time be observed between lidar and met-mast observed wind speeds, in particular near hub height (59 m).

In Fig. 7 we inter-compare 3-hours of wind speed measurements from the lidar with the corresponding measurements from a cup anemometer installed in the met mast close to hub height. The wind speed measurements are seen to correlate well the first 2½ hours before the wind speed drops and the wind direction changes such that it is likely that the met-mast is affected by a wake of a turbine. It can also be seen that the lidar smoothes out the high-frequency variability due to the spatial filtering effects caused by the lidar's finite measuring volume [5, 6].

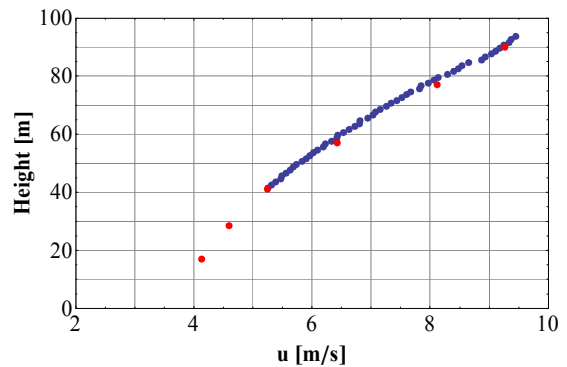


Figure 6: Comparison of a lidar-measured 10-min averaged vertical wind profile (purple dots) with data from a co-located adjacent instrumented MET-mast (red dots).

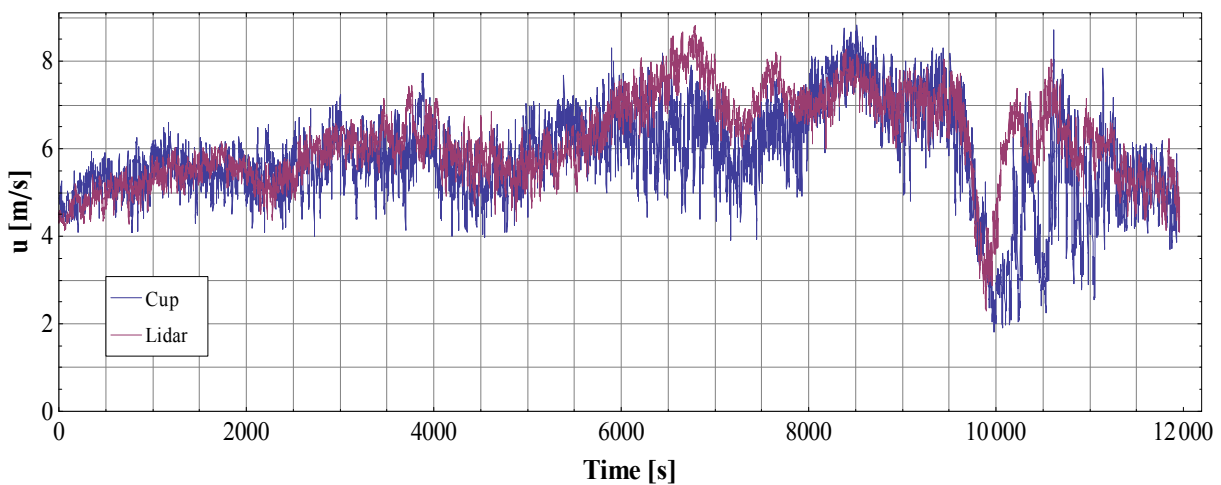


Figure 7: Spinner-lidar measured wind speeds near hub height (purple curve) inter-compared with cup anemometer measured wind speeds in the met mast (blue curve), during a 3-Hour data sampling period on the night of April 30, 2009. Data rate for lidar = 50Hz; Data rate for mast = 10Hz.

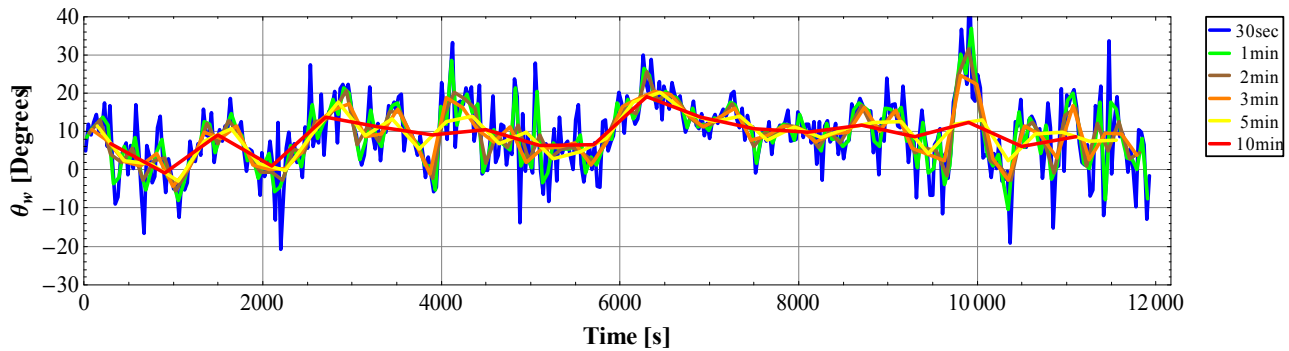


Figure 8: Wind turbine yaw error (θ_w) relative to the mean wind direction measured by the lidar. Yaw-errors shown for six different averaging times (30sec, 1min, 2min, 3min, 5min, and 10min).

3.2 Yaw Error Data Analysis

The wind turbine's yaw error (or horizontal misalignment) has been calculated as a function of time as the difference between the horizontal wind direction determined in the upwind rotor plane from data from the spinner-mounted wind lidar at hub height (± 2.5 m) and the wind turbine's instantaneous pointing direction or Yaw orientation. To determine the instantaneous yaw error we applied the model described in Appendix A). The result is shown in Figure 8.

While the 10-min average yaw error is limited to within the interval -1 to +20 degrees during the 3.33 hour long test period, the short-term averaged yaw-error was measured to exhibit deviations by as much as -20 to +40 degrees.

3.3 Lidar Measured Power Curves

Lidar-measured Power curves have been performed on the same-screened subset of wind data as shown in Figure 8 above, that is, only unobstructed wind directions have been included. Lidar wind data were extracted from azimuth scans near the hub-height ± 2.5 m using the coordinate transformation methodology described in Appendix A.

To eliminate possible wake effects from the turbine to influence the MET-tower cup wind speed measurements the power curves presented have furthermore been screened so only periods where the wind directions were between 20 – 30 degrees (NNE), i.e. only un-obstructed flow to the MET tower has been included.

The 1.34 \varnothing forward-looking spinner-mounted wind lidar proved capable of providing wind speed data for power curve calculations that resemble cup-

anemometer based wind speed based power curves, see Figure 9.

The scatter in the power curves increases as expected with decreasing averaging times. The wind-lidar determined power curve based on 1-s averaged wind data show less scatter than does the corresponding cup-anemometer based power curve. Since we already have screened the data to avoid contamination from wakes this increased scatter may be caused by the longer separation between the MET-mast and the turbine (distance $\sim \varnothing 3.75$), whereas the wind lidar with the 15-degree wedge in this case measured the wind speed at only 103 meters upwind from the turbine. In addition, the wind lidar averages the wind speed more effectively than does the cup anemometer due to the scanning of the beam and the wind lidar's larger radial sampling length, in this case of order 20-m.

4 Discussion

4.1 Perspectives

Upwind lidar measurements integrated with active pitch control

We have demonstrated that a contemporary spinner-mounted CW lidar can measure wind turbine axial wind components upwind at multiple sampling points distributed over the rotor plane of an operating wind turbine.

When combined with the control systems of the turbine, we envision that such measurements can provide real-time control data to the turbine's individual blade pitch control (IPC) systems, and in this way help compensate the effects of yaw errors and strong wind shear and veer.

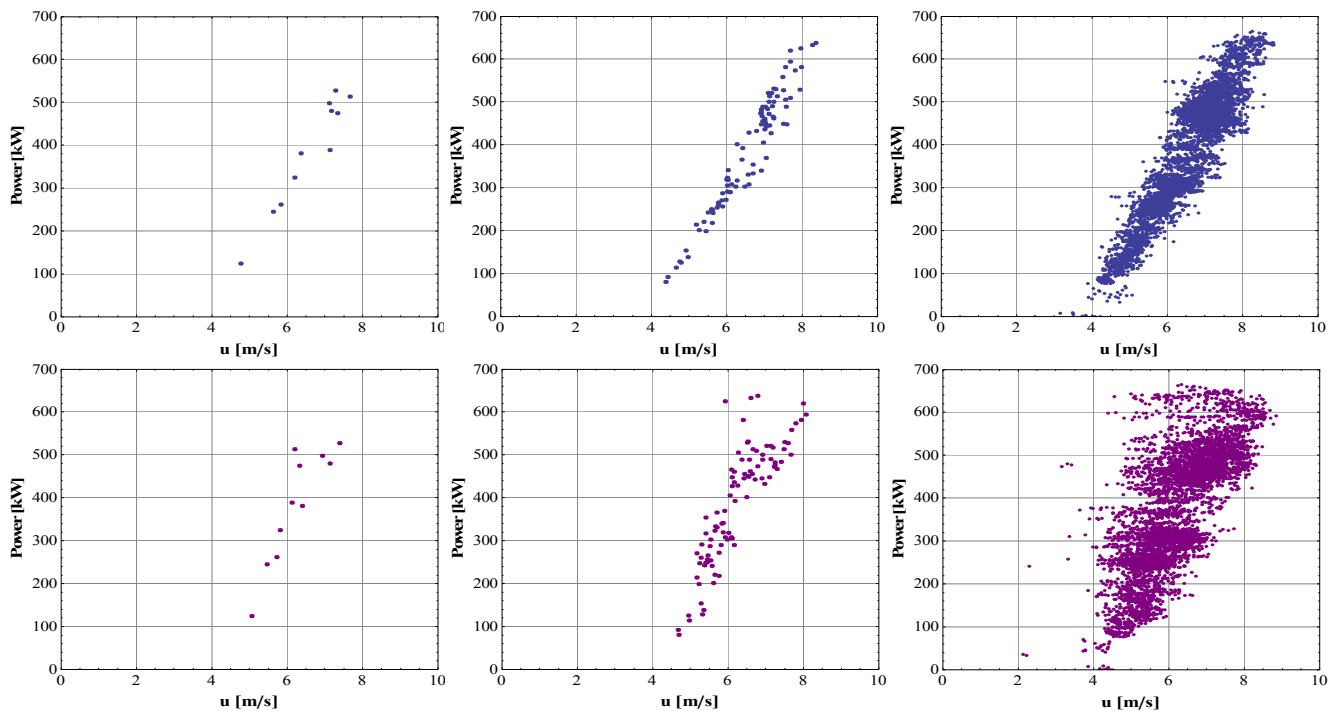


Figure 9: Power curves determined from lidar-measured horizontal wind speed 1.24 Ø upwind (upper panel) compared with simultaneous measured power curves based on a hub-height cup anemometer (lower panel). Power curves are shown for: 10-min (left), 1-min (middle) and 1-s (right) averages.

We also envision that such wind data in combination with an active IPC system can help increase the power production of the turbine during sub-rated wind regime operation. This is to be demonstrated in practice in forthcoming experiments.

5. Conclusions

We report what we believe are the first spinner-based lidar measured wind speeds sampled from the rotating frame of an operating wind turbine.

The “Tjæreborg Spinner-lidar Experiment” has demonstrated that a contemporary cw wind lidar (ZephIR) when mounted in the turbine spinner is able to measure the upwind approaching wind and turbulence structures from scanning the wind field about the turbine axis in real time. The spinner-integrated wind lidar system has shown excellent reliability and data availability was very high throughout the measurement period from the beginning of April through August 2009.

We have shown here that a wind turbine’s instantaneous yaw-error can be measured in real-time. Also we have shown that a wind turbine’s power curves can be measured based on the radial wind measurements from a spinner-mounted wind lidar.

These, our first results, including the aforementioned first analysis of the data from April 30, 2009 now further encourage more analysis of data already sampled during the Tjæreborg Spinner Experiment but also development and integration of wind lidar technologies in the area of active control and improvement of wind turbine performance.

The next stages of development will involve further data analysis and also modeling and incorporation of lidar data as input to the wind turbine’s yaw and pitch control systems, leading to a quantitative assessment of the potential for turbine performance improvement.

References

- [1]. Harris, M., M. Hand and A. Wright, “A Lidar for turbine control”, Tech. Rep. NREL/TP-500-39154 National Renewable Energy, National Renewable Energy Laboratory, NREL, Golden, Colorado, US, (2006).
- [2]. Harris M., D .J. Bryce, A. S. Coffey, D. A. Smith, J Birkemeyer & U Knopf, “Advance measurement of gusts by laser anemometry”, *J Wind Eng.* 95, 1637-1647 (2007).
- [3]. Karlsson, K., F. Olsson, D. Letalick & M. Harris, “All-fiber multifunction CW 1.55 micron

coherent laser radar for range, speed, vibration and wind measurements”, *Applied Optics*, 39, 3716-3726 (2000).

- [4]. Smith, D. A., M. Harris M, A. S. Coffey, T. Mikkelsen, H. E. Jørgensen, J. Mann and R. Danielian, “Wind Lidar Evaluation at the Danish Wind Test Site in Høvsøre”, *Wind Energy*, 9, 87-93 (2006).
- [5]. Sjöholm, M., T. Mikkelsen, J. Mann, K. Enevoldsen, M. Courtney, “Spatial averaging-effects on turbulence measured by a continuous-wave coherent lidar”, *Meteorologische Zeitschrift* 18, 281-287 (2009).
- [6]. Mikkelsen, T. “On mean wind and turbulence profile measurements from ground-based wind lidar’s: limitations in time and space resolution with continuous wave and pulsed lidar systems”. Presented at: 2009 European Wind Energy Conference and Exhibition. Marseille (FR), 16-19 Mar, 2009. In: *EWEK 2009 Proceedings* (online): Wind Profiles at Great Heights, p. 10 pages EWEK (2009).
- [7]. Mikkelsen, T., C. Michael; I. Antoniou, J. Mann. “WindScanner: A full-scale laser facility for wind and turbulence measurements around large wind turbines”. Presented at: *2008 European Wind Energy Conference and Exhibition*. Brussels (BE), 31 Mar - 3 Apr 2008 In: Conference proceedings (online), p. 10 pages EWEK (2008).

Appendix A

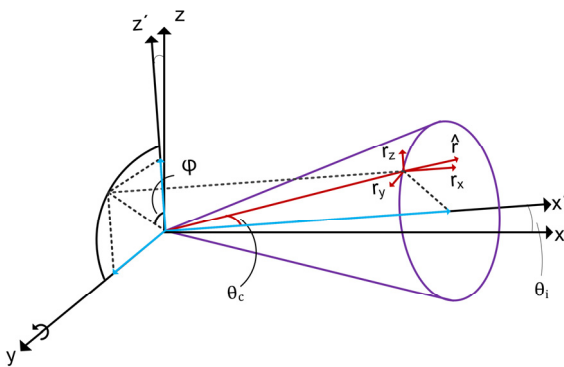


Figure A1: Geometry of the spinner-mounted wind lidar pointing vector in a fixed frame of reference on the ground and in a frame of reference aligned with the wind turbine’s axis of rotation.

The spinner-mounted wind lidar acquires radial wind speed measurements by conical scanning

about the wind turbine’s axis of rotation, which in the horizontal plane is steered by the wind turbine yaw control and the vertical direction is elevated a fixed angle, θ_i (5 degrees for the NM80 wind turbine).

The lidar measures the wind speed projected along the lidar’s instantaneous line-of-sight unit pointing vector, here denoted by \hat{r} , and is given by

$$\begin{aligned} \hat{r} &= (r_x, r_y, r_z) \\ &= (\cos \theta_c, \sin \theta_c \sin \varphi, \sin \theta_c \cos \varphi) \end{aligned} \quad (1)$$

where the lidar’s fixed off-turbine axis deflection angle is denoted θ_c (15 or 30 degrees in this study) and the azimuth angle caused by rotation of the lidar’s prism is denoted φ .

In this tilted and yawed coordinate system the measured wind speed is

$$U_{Lidar} = \hat{r} \cdot \mathbf{u} = (r_x, r_y, r_z) \cdot (u_x, u_y, u_z) \quad (2)$$

where (u_x, u_y, u_z) are the wind components of the instantaneous wind vector in the frame of reference attached to the ground. We assume that the mean wind direction is along the x-axis.

To relate the line-of-sight pointing vector \hat{r} in the tilted and yawed reference system to the fixed frame of reference for the wind vector we first had to apply the following two coordinate rotations:

i) Relative to a fixed coordinate system attached to the ground (x, y, z) the vertical tilt of the wind turbine axis is represented by a counter-clockwise rotation about the y-axis:

$$\begin{bmatrix} x' \\ y' \\ z' \end{bmatrix} = \begin{bmatrix} \cos \theta_i & 0 & \sin \theta_i \\ 0 & 1 & 0 \\ -\sin \theta_i & 0 & \cos \theta_i \end{bmatrix} \begin{bmatrix} x \\ y \\ z \end{bmatrix} \quad (3)$$

ii) Similarly, the yaw-error of the wind turbine, θ_w , relative to the x-axis is taken into account by rotation around the z- axis, viz.:

$$\begin{bmatrix} r_x \\ r_y \\ r_z \end{bmatrix} = \begin{pmatrix} \cos \theta_w & \sin \theta_w & 0 \\ -\sin \theta_w & \cos \theta_w & 0 \\ 0 & 0 & 1 \end{pmatrix} \begin{bmatrix} x' \\ y' \\ z' \end{bmatrix} \quad (4)$$

From Eqs (3) and (4) an expression for the lidar's instantaneous radial wind speed is derived by relating the pointing vector \hat{r} in Eqs. (1) to the fixed frame as function of tilt, azimuth, wedge deflection angle and yaw.

Acknowledgements

Mikael Rasmussen and Per Hansen of Risø DTU, and Dong Energy are gratefully acknowledged for skilled technical support and for access to the NM80 test Turbine at Tjæreborg, Vestas Winds Systems is acknowledged for safe operations in the NM80 Turbine. The lidar-in-spinner experiment has been conducted as part of the new Danish research infrastructure facility activities under the auspices of Windscanner.dk [7]. Access to DONG Energy's NM80 Tjæreborg wind turbine and the local met-mast data has been facilitated in collaboration with the simultaneously ongoing DAN-AERO and TOPFARM test activities which is also gratefully appreciated.

Meteorology and turbine data was provided by the DAN-AERO MW project, carried out by Vestas, Siemens, LM, DONG Energy and Risø DTU in cooperation and funded partly by EFP-2007, "Experimental Rotor- and Airfoil Aerodynamics on MW Wind Turbines" contract nr. 33033-0074 and partly by the participants.

Contact

If you have any queries, or technical or conceptual comments, please do not hesitate to contact the corresponding authors.